Pergamon

Tetrahedron Vol. 51, No. 32, pp. 8901-8914, 1995

0040-4020/95 $9.50+0.00

0040-4020(95)00499-8

Halex Exchange and Fluorodenitration Transition State Structures and Energies - Semiempirical Study with AM1, SAM1 and PM3.

Timothy Smyth* and, in part, Aedin Carey

Department of Chemical and Environmental Sciences, University of Limerick,
National Technological Park, County Limerick, Ireland.

Abstract: The potential energy surfaces for the halex exchange and fluorodenitration reactions of 2,4-dichloronitrobenzene, with free fluoride ion and with tetramethylammonium fluoride, have been studied using AM1, SAM1, and PM3 semiempirical methodologies. A number of interactions were observed between the aromatic substrate and tetramethylammonium fluoride which are viewed as being reaction path determinants between the competing processes.

INTRODUCTION

We report here on a semiempirical study of the halex exchange and fluorodenitration reactions of 2,4-dichloronitrobenzene (DCNB). We have recently examined experimentally the halex exchange conversion of DCNB to 2,4-difluoronitrobenzene (DFNB).[1] In the experimental work it was found that a quaternary ammonium ion played a key catalytic role, that the *o*-Cl group of DCNB was displaced more rapidly (by up to a factor of 3) than the *p*-Cl group (Scheme 1) and no fluorodenitration[2] products were observed. It is clear that the quaternary ammonium ion must function to extract the fluoride ion (from the solid KF) and must also be involved in the addition of fluoride ion to the aromatic substrate. In this latter process it is meaningful to ask what role the quaternary ammonium-fluoride complex plays in the observed faster reaction at the ortho position and what differences arise in the reaction profile of the halex exchange and fluorodenitration processes. To this end the potential energy surface of the halex exchange and fluorodenitration reactions of DCNB was studied using a variety of semiempirical methodologies (SAM1, AM1 and PM3). Two fluoride ion sources were compared in this study *viz.*, tetramethylammonium fluoride (TMAF) and free fluoride ion. The interactions between TMAF and the substrate are likely to be distinct from those with free fluoride ion and more relevant to patterns of reactivity in solution insofar as TMAF could be regarded as a very specifically solvated form of fluoride ion. Solvent effects are very important for both halex exchange and fluorodenitration reactions. Clark *et al.* has observed that the solvent can play a significant role in determining which reaction type predominates where these processes compete.[2a] In this study, however, we have concentrated on probing the fundamental interactions of the reactant species as a reference starting point.

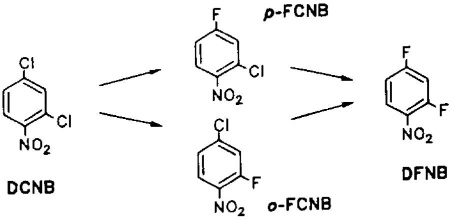

Scheme 1

Procedure

The calculations were carried out using AMPAC 5.0[3] on a DEC 3000/400 workstation. Standard SAM1, AM1 and PM3 parameters were used. Full geometry optimisation of the neutral substrates and the Meisenheimer intermediates was carried out by minimising the energy using the default method in the programme (DFP/BFGS) without any symmetry or geometry constraints. The keyword PRECISE was used in all calculations; in general all the gradient norms obtained were well within required criteria. Initial searches for potential transition states was carried out by the reaction coordinate method. Thus within the Meisenheimer intermediates the C-F or C-Cl bond length, as appropriate, was incremented by 0.2 Å and the enthalpy of formation determined. A structure located in this way close to an energy maximum was then further refined using gradient minimisation via the LTRD method which is a standard feature of the programme. All transition states reported here had a single negative eigenvalue and were tracked through to chemically correct left and right minima, using the transition vector with the PATH option in the programme; in the majority of cases the PATH operation gave fully optimised structures for the left and right minima but occasionally further energy minimisation was required to get a fully optimised structure. The minima identified in this way involving the neutrals (DCNB, *o*-FCNB, *p*-FCNB and DFNB) in combination with the halide anions corresponded to ion-molecule complexes. This is to be expected as the separated components will not form discrete minima on the potential energy surface in the gas phase; ion-molecule complexes involving the halide anions are well known.[4] The barrier to rotation in the transition states was evaluated by two different approaches. In one approach (method a) all the structural parameters for a transition state structure (located as outlined above) were fixed and the NO_2 dihedral angle was incremented through 180° by 15° intervals; in the second approach (method b) the dihedral of the nitro group was fixed at 90° to the aromatic ring in the Meisenheimer intermediate and the transition state structure was located from this starting point in the standard manner as outlined above.

RESULTS AND DISCUSSION

Enhanced *ortho* reactivity has been noted before in a variety of nucleophilic aromatic displacement reactions[5] and has led to a number of putative explanations. One rationale is that the nitro group cannot achieve coplanarity with the aromatic ring because of steric blocking by the *o*-Cl group. This should leave the nitro group largely exerting an inductive effect, which, decreasing in strength with increasing distance from the reacting centre activates the adjacent *o*-Cl more than the *p*-Cl group.[6] While intuitively attractive and simple this explanation has so far not been substantiated; it would require that the barrier to rotation of the nitro group be such that the conformer with the nitro group coplanar with the aromatic ring be very non populous not only in the ground state but also in the transition state. Politzer *et al.* have examined the role of electrostatic potential of the nitro group using ab initio calculations.[7] They noted a build-up of positive potential above the nitro group, when this is coplanar with the aromatic ring, and postulated that this could serve as a pathway for nucleophilic attack particularly at an adjacent *ortho* position. Rotation of the nitro group away from coplanarity with the ring reduced the positive potential considerably. In a kinetic study of the reaction of *o*- and *p*-chloronitrobenzenes with piperidine Bunnett and Morath found that the *o*-Cl group is displaced faster than the *p*-Cl group.[5] A detailed study by these authors revealed that the *ortho*:*para* ratio of rates varied systematically with the solvent polarity. This finding, together with an analysis of the variation in entropy of activation with solvent polarity for the *o*-Cl versus *p*-Cl displacement, pointed very clearly towards a direct electrostatic or polar interaction in the transition state between the piperidine nucleophile and the nitro group in the *o*-chloronitrobenzene structure. This interaction as described by Bunnett and Morath along with the SAM1 fully characterised transition state structure obtained here is shown in Figure 1.

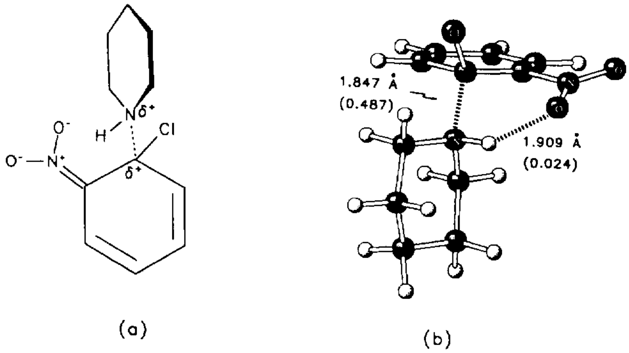

Figure 1. Transition state structures for displacement of an ortho chloro group by piperidine as (a) depicted by Bunnett and Morath[5] and (b) as characterised by SAM1; the numbers in parenthesis are bond orders.

This latter view shows the polar H on the piperidine nitrogen interacting with an oxygen of the nitro group while the former picture is less explicit in this aspect. This type of "internal" solvation, which is not possible with *p*-chloronitrobenzene, was thus viewed as playing an important role in the enhanced reactivity at the *ortho* position.

The Potential Energy Surface with free F^-. - The AM1 heat of formation for F^- is considerably in error compared with the experimental value[8] (Table 1) while the SAM1 and PM3 values are closer to the experimental value they, nonetheless, deviate significantly from this. There must be some errors in the calculated enthalpies of formation of the transition states where the fluoride ion species retains a large degree of ionic character. As the analysis of the data here is through comparative rather than via absolute values the trends observed should provide a meaningful insight to the reaction surfaces.[9]

Table 1. Calculated and experimental enthalpies of formation of miscellaneous species.

Structure	SAM1	AM1	PM3	Expt'l[8]
F^-	-32.38	3.44	-31.23	-59.9
Cl^-	-41.77	-37.66	-51.23	-55.9
TMA[+a]	135.44	157.13	154.09	
TMAF[b]	-27.86	-14.59	-31.16	

a) Tetramethylammonium ion; b) tetramethylammonium fluoride.

There are significant differences in the enthalpies of formation as determined by the various Hamiltonians for the different structures, however, the trends are quite consistent (Table 2). The barrier to rotation of the nitro group in the neutral state structures is quite similar for SAM1 and AM1. The energy maximum occurs with AM1 when the nitro group is exactly coplanar with the ring (a lower maximum occurs at 90°) whereas this occurs with SAM1 when the nitro group is at 90° to the ring (a lower maximum occurs at 180°). Interestingly both SAM1 and AM1 give a higher barrier for those structures with a fluorine in the ortho position compared to a chlorine: in each case the energy maximum occurs when the nitro group is perpendicular to the ring. With PM3 the barrier is fairly constant for all the neutral structures. A much larger dipole is assigned to the nitro group by PM3 compared to SAM1 and AM1 (the atomic charges on N and O respectively are +1.31 and -0.58 (PM3), +0.68, -0.40 (SAM1) and +0.57, -0.35 (AM1)). The barrier to rotation of the nitro group in nitrobenzene has been determined experimentally, using microwave spectroscopy,[10] to be between 2.8 and 3.3 kcal mol^{-1} while the calculated values are 2.16 (SAM1), 3.48 (AM1) and 1.63 kcal mol^{-1} (PM3). Thus it would appear that both SAM1 and AM1 give good estimates for the rotation barrier whereas the PM3 value is too low.

Table 2. Data on optimised geometries for neutral structures and halex type Meisenheimer intermediates and transition states involving free F^-.

	ΔH^0_f kcal mol^{-1}			NO_2 twist angle[a]			NO_2 rotation barrier[b]		
Structure	**SAM1**	**AM1**	**PM3**	**SAM1**	**AM1**	**PM3**	**SAM1**	**AM1**	**PM3**
DCNB	3.52	18.22	5.61	37.11	45.02	33.63	0.64	0.86	0.93
o-FCNB	-34.32	-21.86	-31.67	0.05	0.15	33.54	2.58	2.60	0.91
p-FCNB	-31.64	-19.76	-30.97	30.00	30.00	30.00	0.78	0.66	1.00
DFNB	-69.65	-60.11	-68.19	0.00	-0.03	30.00	2.83	2.78	0.94
Meisenheimer Intermediates									
DCNB (*ortho* add'n)	-85.55	-83.50	-104.06	6.28	0.33	-1.64	9.59	8.70	6.08
DCNB (*para* add'n)	-85.06	-82.33	-104.55	0.29	-5.64	-2.12	7.56	5.77	5.47
o-FCNB (*para* add'n)	-121.81	-124.25	-144.09	-0.13	0.11	-1.55	9.71	8.83	5.90
p-FCNB (*ortho* add'n)	-118.67	-121.99	-141.95	-6.68	0.31	1.57	9.78	8.77	6.23
Transition States (F^- addition)									
DCNB (*ortho* add'n)	-33.24	3.95	-40.31	2.01	19.26	-27.04	4.75[c]/3.98[d]	3.61[c]/2.46[d]	3.65[c]/3.05[d]
DCNB (*para* add'n)	-33.26	4.83	-39.79	12.01	-31.90	13.82	3.51[c]/1.60[d]	2.12[c]/----[d]	2.31[c]/1.33[d]
o-FCNB (*para* add'n)	-70.04	-35.79	-78.56	3.24	-1.84	12.27	5.20[c]/3.60[d]	4.16[c]/3.11[d]	2.45[c]/1.47[d]
p-FCNB (*ortho* add'n)	-66.03	-33.76	-77.89	-1.72	16.92	-26.63	4.57[c]/6.12[d]	3.62[c]/4.54[d]	3.75[c]/3.11[d]
Transition States (Cl^- loss)									
DCNB (*ortho* loss)	-74.78	-72.12	-95.20	0.87	-7.29	-32.57	-	-	-
DCNB (*para* loss)	-71.49	-68.77	-94.23	18.66	32.96	-15.43	-	-	-
o-FCNB (*para* loss)	-108.92	-109.82	-132.76	-0.49	2.29	-14.45	-	-	-
p-FCNB (*ortho* loss)	-107.80	-109.47	-132.60	0.04	7.02	32.45	-	-	-

a) The dihedral angle (degrees) of the NO_2 group to the aromatic ring ; b) kcal mol^{-1}

c) Method a - see procedure section; d) Method b - see procedure section.

The barrier to rotation in the Meisenheimer intermediates is calculated to be significantly higher and the nitro group is seen to be essentially coplanar with the aromatic ring in all cases. Delocalisation of part of the negative charge, by resonance, onto the nitro group is important for stability as there is now one full negative charge on the system. The extent of charge transfer from the fluoride ion to the aromatic nucleus in the transition state is quite low, nonetheless, it would appear that delocalisation of this charge over the nitro group, is important. Thus the barrier to rotation of the nitro group in the transition states is, in general, higher than that in the corresponding neutral structure although lower than for the Meisenheimer intermediates. With

SAM1 the nitro group is seen to be coplanar, or very close to being coplanar, with the aromatic ring in the transition states, however, with AM1 and PM3 this is generally not the case indicating that resonance onto the nitro group is not necessarily the dominant interaction as seen by these Hamiltonians. The SAM1 transition state structure for F^- addition is shown in Fig.2 (a). The AM1 and PM3 transition state structures are similar to those in Fig.2 (a) with the following values for C···F bond length and fluoride ion charge: 2.381 Å, -0.777 (AM1), 2.605 Å and -0.964 (PM3).

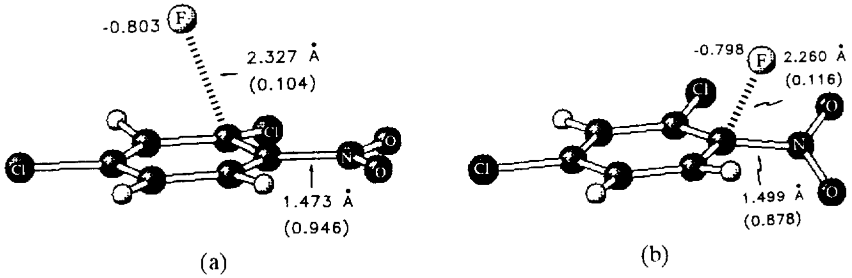

Figure 2. SAM1 transition state structures for (a) halex exchange and (b) fluorodenitration reactions of DCNB with free fluoride ion; the numbers in parenthesis are bond orders and the signed numbers are atomic charges.

The activation enthalpies for the various F^- addition and Cl^- loss steps are listed in Table 3. These are given as the difference between $\Delta H°_f$ of the transition state and the separated reactants where the experimental values for F^- and Cl^- were used.[8] The AM1 activation values are the largest while the PM3 ones are the lowest. Also PM3 shows the smallest difference in $\Delta H^{\neq}$ between fluoride addition and chloride elimination. The data shows that with each Hamiltonian there is no real difference in $\Delta H^{\neq}$ for addition of free F^- to the *ortho* and *para* positions of the aromatic substrates. For this reaction a reasonably consistent pattern is observed by each of the semiempirical methodologies. This is not quite the case for the fluorodenitration process.

Table 3. Enthalpies of activation (kcal mol^{-1}) for halex reactions of DCNB, *o*-FCNB and *p*-FCNB.

	F^- addition						Cl^- loss					
	ortho			para			ortho			para		
Structure	SAM1	AM1	PM3	SAM1	AM1	PM3	SAM1	AM1	PM3	SAM1	AM1	PM3
DCNB	23.14	45.63	13.98	23.11	46.51	14.50	10.77	11.38	8.86	13.57	13.56	10.33
o-FCNB				24.18	45.97	13.01				12.89	14.43	11.33
p-FCNB	25.22	45.24	12.76				10.88	12.52	9.35			

Fluorodenitration Reaction with Free F^-. Fully characterised transition states were obtained with all the Hamiltonians for the fluorodenitration of DCNB (the SAM1 transition state structure is shown in Fig.2 (b)). In the case of SAM1 and AM1 the fluorodenitration process followed a concerted reaction pathway and no Meisenheimer type addition structure was located as a stable intermediate. In contrast, with PM3 a stepwise reaction pathway was observed proceeding via an addition intermediate. The rate limiting step, however, was loss of NO_2^-. (With nitrobenzene PM3 also showed a stepwise process for the fluorodenitration process although the fluoride ion addition step was slowest; here AM1 and SAM1 showed a concerted reaction). The enthalpies of formation of the halex and the fluorodenitration transition states can be compared directly (Table 4) as the same components are present in each case.

Table 4. Enthalpies of formation for DCNB transition state structures for halex exchange and fluorodenitration with free fluoride ion.

	Halex exchange		Fluorodenitration
	ortho	para	
SAM1	-33.24[a]	-33.26[a]	-29.20[b]
AM1	3.95[a]	4.83[a]	5.99b
PM3	-40.31[a]	-39.79[a]	-46.40[c]

a) Stepwise mechanism, rate limiting addition of F^-; b) Concerted reaction; c) Stepwise mechanism, rate limiting loss of NO_2^-; value given above refers to the fluoride addition step.

The SAM1 values indicate that there is a clear preference (by ~ 4 kcal mol^{-1}) for the halex exchange reaction over fluorodenitration. The AM1 values give a similar indication but the preference is less pronounced (1 - 2 kcal mol^{-1}). The PM3 values on the other hand indicate that addition of fluoride to the nitro carbon is favoured over addition to a halo carbon. Although PM3 shows a stepwise process with rate limiting loss of NO_2^- the activation enthalpy for this step (11.35 kcal mol^{-1}) is lower than that for the corresponding halex exchange reactions (Table 3: 13.98 and 14.50 kcal mol^{-1} *ortho* and *para* respectively).

Tetramethylammonium Fluoride as the Fluoride Ion Source- Anhydrous tetramethylammonium fluoride (TMAF) has been prepared by Christe *et. al.*[11] and a number of its physical and chemical properties determined although molecular structural data was not obtained. A key chemical property is its highly basic character evidenced by the fact that TMAF readily deprotonates acetonitrile. In fact ^{19}F NMR data indicated that TMAF interacted strongly with most solvents in which it was soluble.[11] The SAM1, AM1 and PM3 optimised structures for TMAF obtained here are shown in Figure 3.

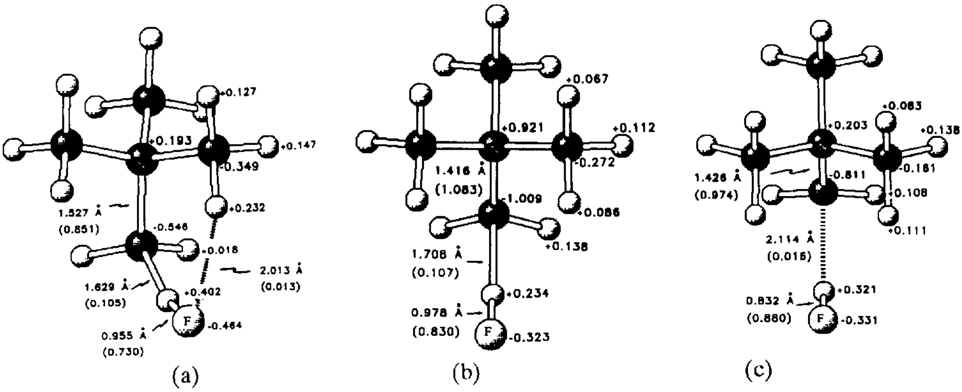

(a) (b) (c)

Figure 3. Structure of TMAF (a) SAM1, (b) PM3 and (c) AM1; the numbers in parenthesis are bond orders and the signed numbers are atomic charges.

The optimised structure in each case is best described as a complex of HF and a trimethylammoniummethylene ylide, although, there are some differences in charge distribution within these. The fluoride is strongly bonded to one hydrogen, and, in the case of SAM1 only, is weakly interacting with another. It is clear that this structure can only refer to an isolated gas phase TMAF molecule, although, there is good experimental evidence on the tendency of F^- to interact strongly with a hydrogen atom in a polar bond in condensed phases.[11, 12] Thus Christe *et. al.* obtained the crystal structure of an adduct, involving TMAF and a dimer derived from acetonitrile, in which a strong interaction between F^- and two N-H bonds was observed.[11]

Two transition state structure types were located with TMAF as the fluoride ion source. One involved F^- as the atom in flight and resulted in the normal Meisenheimer adduct; such a transition state was fully characterised by both SAM1 and PM3 but not with AM1. The second type of transition state structure involved TMAF as the entity in flight. This was fully characterised by both AM1 and PM3 but not with SAM1. With AM1 the transfer resulted in the addition of TMAF to the aromatic substrate: this was considerably less stable than the adduct of F^- at the same position. With PM3 the transfer resulted in the normal Meisenheimer adduct of the aromatic substrate and F^-. The relevant data is summarised in Table 5. The activation enthalpies (taken as the differences in enthalpy between the transition state and the separated reactants) for the various reactions are listed in Table 6. The SAM1 values show a clear preference for delivery of F^- from TMAF to the *ortho* position compared to the *para* position both for DCNB and for the monofluorochloronitrobenzene isomers. The PM3 values for the same type of process are almost identical for *ortho* and *para* delivery. In the case of the process involving TMAF as the moiety in flight both the AM1 and PM3 values indicate a clear preference for delivery to the *ortho* position.

Table 5. Enthalpies of formation (kcal mol^{-1}) of optimised geometries for halex type Meisenheimer intermediates and transition states involving TMAF.

Structure	SAM1	AM1	PM3	SAM1	AM1	PM3
Meisenheimer Intermediates		F$^-$ adduct^{a}			TMAF adduct	
DCNB (*ortho* add'n)	-25.96	-3.52	-37.52	---	31.21	---
DCNB (*para* add'n)	-11.39	6.37	-24.52	---	38.82	---
p-FCNB (*ortho* add'n)	-60.31	-42.20	-74.78	---	-7.56	---
o-FCNB (*para* add'n)	-48.84	-34.55	-63.32	---	-2.51	---
Transition States		F$^-$ transfer			TMAF transfer	
DCNB (*ortho* add'n)	7.75	---	1.96	---	35.69^{b}	4.41^{c}
DCNB (*para* add'n)	10.55	---	2.50	---	40.44^{b}	8.41^{c}
p-FCNB (*ortho* add'n)	-26.85	---	-35.44	---	-3.06^{b}	-31.92^{c}
o-FCNB (*para* add'n)	-27.15	---	-36.23	---	-0.29^{b}	-30.28^{d}

a) Includes an associated TMA$^+$ counter ion; b) TMAF transfer leading to TMAF adduct; c) TMAF type transfer leading to fluoride ion adduct; d) Concerted reaction.

Table 6. Enthalpies of activation (kcal mol^{-1}) for the halex reaction of TMAF with DCNB, *o*-FCNB and *p*-FCNB .

	F$^-$ transfer						TMAF transfer					
	ortho			para			ortho			para		
Structure	SAM1	AM1	PM3	SAM1	AM1	PM3	SAM1	AM1	PM3	SAM1	AM1	PM3
DCNB	32.09	---	27.51	34.89	---	28.05	---	32.06^{a}	29.96^{b}	---	36.81^{a}	33.96^{b}
o-FCNB				35.02	---	26.60				---	36.16^{a}	32.55^{b}
p-FCNB	32.65	---	26.69				---	31.29^{a}	30.21^{c}			

a) TMAF transfer leading to TMAF adduct; b) TMAF type transfer leading to fluoride ion adduct; c) Concerted reaction.

The PM3 set of data alone allows a comparison to be made between the two types of process and it is clear that the process involving F$^-$ as the atom in flight is consistently more favourable than that involving TMAF.

The SAM1 transition state structures involving the transfer of F$^-$ from TMAF to the *ortho* and *para* positions of DCNB are shown in Fig. 4 (a) and (b) and the AM1 *para* transition state is shown in Fig. 4 (c). Although there are similarities in terms of bond lengths and atomic charges in the transition states involving F$^-$ as the atom in flight, there are also some significant differences in the types of interactions occurring between TMA$^+$ and the aromatic structure.

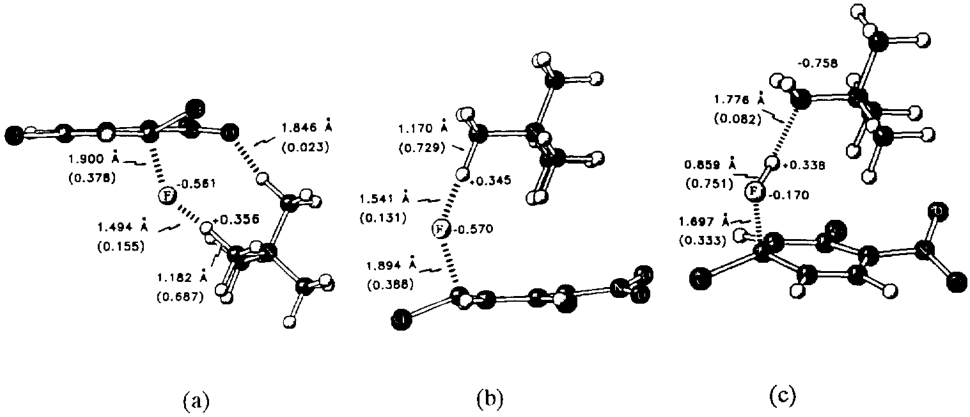

Figure 4. Halex exchange transition state structures (SAM1) of DCNB with TMAF, (a) *ortho*, (b) *para* and (c) the AM1 *para* transition state with TMAF as the entity in flight.

Thus in the *ortho*-transition state structure a stabilising electrostatic interaction is seen to occur between an oxygen of the nitro group and a hydrogen atom of TMA$^+$. This interaction is reminiscent of the "internal" solvation proposed by Bunnett and Morath[5] outlined earlier (Figure 1) and, although here a polar CH bond rather than an NH one is involved, there is good experimental evidence for this type of interaction between TMA$^+$ and a variety of polar molecules in the gas phase.[13] The enthalpy of interaction between TMA$^+$ and DCNB (through the polar nitro group) is 18.91 (SAM1), 13.82 (AM1) and 17.75 kcal mol^{-1} (PM3). A similar type of polar interaction is not possible for the *para* transition state, however, a somewhat weaker interaction between TMA$^+$ and the aromatic π cloud does occur. This is apparent from the orientation of TMA$^+$ over the aromatic ring: the separation of the ammonium N atom and the centre of the aromatic ring is about 4.48 Å (SAM1) 4.30 AM1 and 4.30 Å (PM3). The enthalpy of the interaction of benzene and TMA$^+$ is calculated to be 4.87 (SAM1), 4.30 (AM1) and 10.93 kcal mol^{-1} (PM3) with contact distances as defined above of 4.37 (SAM1), 4.07 (AM1) and 4.02 Å (PM3). The interaction between benzene and TMA$^+$ been studied experimentally[13] and theoretically.[14, 15] The enthalpy of interaction has been experimentally determined to be 9.4 kcal mol^{-1} in the gas phase.[13] (The relevance of this type of TMA$^+$ interaction with aromatic residues has been demonstrated in the binding of quaternary ammonium groups within hydrophobic pockets in proteins[16] and in water soluble macrocycles[17]). It would appear that both SAM1 and AM1 underestimate this interaction whereas PM3 gives a reasonably good estimate; the under evaluation of this interaction in the para transition state would result in giving this process a less favourable activation enthalpy than was warranted. Nonetheless, a reasonably consistent picture of ortho activation in the halex exchange reaction by all three semiempirical methodologies emerges.

It is doubtful that a fluoride ion can exist as a free anion in any condensed phase[18] but most likely will occur as an ion-molecule type complex of greater or lesser complexity depending on solvation. It is not unreasonable to consider that the structure of TMAF (Fig. 3) defined by the semiempirical methodologies is a legitimate one. Other interactions may be supplied by a solvation shell, nonetheless, it is likely that the core interaction occurs in the TMAF complex itself and that the interactions between TMAF and the DCNB as outlined above are determinant in the *ortho vs para* halex reaction pathways.

Fluorodenitration Reaction with TMAF. Fully characterised transition state structures were located for the fluorodenitration reaction of DCNB with TMAF by each of the semiempirical methodologies, however, there were considerable differences in the reaction pathways. A fully concerted reaction was observed with SAM1 and AM1 while PM3 showed a stepwise process. The SAM1 transition state involved F^- as the atom in flight. The AM1 transition state involved TMAF as the entity in flight - displacement of the nitrite ion being concomitant with the return of a proton to the tetramethylammonium moiety. These transition state structures are shown in Figure 5.

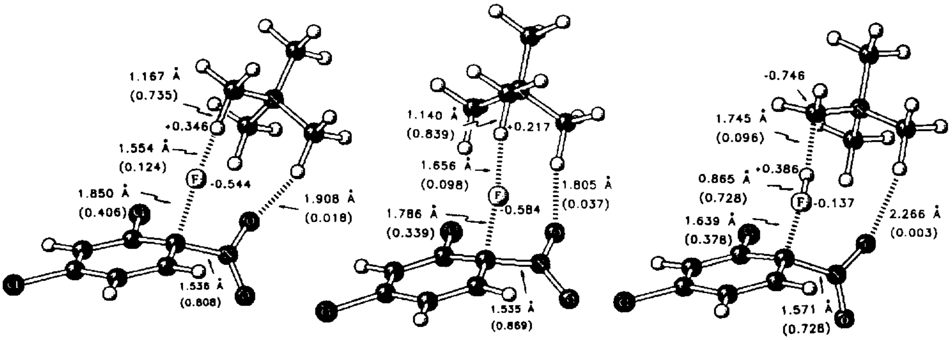

(a) (b) (c)

Figure 5. Fluorodenitration transition state structures of DCNB with TMAF, (a) SAM1, (b) PM3 and (c) AM1.

The enthalpies of formation of the halex and the fluorodenitration transition states can be compared directly (Table 7). The values show that each Hamiltonian indicates a clear preference for halex exchange over fluorodenitration and, as stated earlier the ortho halex exchange is the most favoured.

Table 7. **Enthalpies of formation for DCNB transition state structures for halex exchange and fluorodenitration with TMAF.**

	Halex exchange		Fluorodenitration
	ortho	para	
SAM1	7.75[a]	10.55[a]	14.50[b]
AM1	35.69[c]	40.44[c]	42.35[d]
PM3	1.96[a]	2.50[a]	9.73[a]

a) Fluoride ion addition, stepwise mechanism, rate limiting F^- addition; b) Concerted reaction; c) TMAF transfer process, stepwise mechanism; d) TMAF transfer process, concerted reaction.

Halex exchange vs Fluorodenitration. The differences in the activation enthalpies for *ortho* halex exchange and fluorodenitration of DCNB with TMAF as evaluated by the various Hamiltonians are 6.75 (SAM1), 6.66 (AM1) and 7.77 kcal mol^{-1} (PM3). These values are significant and it is of interest to identify possible features in the relevant transition states which might help rationalise these differences. In both the *ortho* halex and fluorodenitration transition states the TMA^+ moiety interacts with both the F^- which is being transferred and with an oxygen atom of the nitro group. This interaction with the oxygen atom in the ortho halex exchange transition state leaves the nitro group essentially coplanar with the aromatic ring while in the fluorodenitration transition state the nitro group is orthogonal, or close to orthogonal, to the aromatic ring: in the orthogonal orientation a resonance interaction with the developing charge on the ring is not possible. It is also the case that the fluoride ion species is closer to an oxygen atom of the nitro group in the fluorodenitration transition state. This latter interaction is probably not that not significant however. Thus in the AM1 transition state there is quite a low atomic charge on the fluoride yet the difference in activation enthalpy is equally as large as that seen with SAM1 where the fluoride ion charge is much higher. It is possible that appropriately juxtaposed solvent molecules could provide stabilisation of the nitro group, instead of TMA^+, while leaving it in a more favourable orientation in the fluorodenitration reaction: it is not clear, however, that simply allowing the nitro group to remain coplanar with the aromatic ring, via independent solvation, would fully remove the differences in the transition state energies observed above. A more comprehensive study of solvation effects is warranted and in this context it is of interest to note that Clark *et al* has observed that the choice of solvent can play a significant role in determining which reaction type (halex exchange *vs* fluorodenitration) predominates where these processes compete[2a]: reaction of 1,2,4,5-tetrachloro-3-nitrobenzene with TMAF gave a greater degree of fluorodenitration over halex exchange in acetonitrile than in dimethylacetamide.

CONCLUSIONS

Fully characterised transitions states for the halex exchange and fluorodenitration reactions of 2,4-dichloronitrobenzene (DCNB) with free fluoride ion and with tetramethylammonium fluoride (TMAF) have been located using SAM1, AM1 and PM3. All three semiempirical methodologies indicate that there is no clear preference for *ortho* over *para* displacement in halex exchange with free fluoride ion. With free fluoride ion SAM1 indicates a clear preference for halex exchange over fluorodenitration, AM1 indicates the same preference but this is less pronounced while PM3 indicates that fluorodenitration is more favoured than halex exchange. It is clear that any explanation of *ortho* activation in halex exchange, and of the balance between halex exchange and fluorodenitration, must take into account the nature of the nucleophile. For reactions in a condensed phase this will be more complex than free fluoride ion. In this context TMAF can be viewed as a valid minimal complex of fluoride ion and the interactions occurring between it and DCNB are likely to be equal valid; insofar as they indicate that *ortho* halex exchange is preferred over *para* exchange and over fluorodenitration, they concur with our experimental results.[1] A feature which appears to play a key role as a reaction path determinant with TMAF is the interaction of the tetramethylammonium moiety with the nitroaromatic structure. A relatively strong polar type interaction occurs between an oxygen of the nitro group and a polar CH bond of the tetramethylammonium species; this contributes to a stabilisation of the *ortho* halex exchange transition state. A weaker interaction occurs between the ammonium entity and the aromatic π cloud in the *para* halex exchange transition state: this does not provide the same level of stabilisation as that which is part of the *ortho* transition state. The interplay between halex exchange and fluorodenitration in a condensed phase is, however, subject to modulation by the solvent system.[2a] In the fluorodenitration transition states involving TMAF located here an unfavourable orientation of the nitro group is imposed by the TMA^+ moiety; it is possible that this constraint could be removed by independent solvation of the nitro group. More detailed elaboration of the specific role of the solvent as a reaction path determinant awaits further study.

REFERENCES

1 Smyth, T.; Carey, A.; Hodnett, B.K. Tetrahedron, **1995**, *51*, 6363.

2 (a) Clark, J. H.; Wails, D.; Jones, C. W.; Smith, H.; Boechat, N.; Mayer, L. U.; Mendonca, J. S. *J. Chem. Res. (S)*, **1994**, 478; (b) Maggini, M.; Passudetti, M.; Gonzales- Trueba, G.; Prato, M.; Quintily, U.; Scorrano, G. *J. Org. Chem.*, **1991**, *56*, 6406.

3 AMPAC 4.5, © 1993 Semichem, 7128 Summitt, Shawnee, KS 66216

4 (a) Larson, J. W.; Mc.Mahon, T. B. *J. Am. Chem. Soc.*, **1985**, *107*, 766; (b) Jacobson, S; Pizer, R. *J. Am. Chem. Soc.*, **1993**, *115*, 1216.

5 Bunnett, J. F.; Morath, R. J. *J. Am. Chem. Soc.*, **1955**, *77*, 5051.

6 (a) Bunnett, J. F.; Zahler, R. E.; *Chem Revs.*, **1951**, *49*, 322; (b) de Nie-Sarink, M. J.; Prillwitz, P.E. *Spec. Chem.*, 1984, 9

7 Politzer, P.; Lane, P.; Jayasuriya, K.; Domelsmith, L. N. *J. Am. Chem. Soc.*, **1987**, *109*, 1899

8 (a) Woolf, A. A. *Adv. Inorg. Chem. Radiochem.*, **1981**, *24*, 1; (b) Murphy, M. K.; Beauchamp, J. L. *Inorg. Chem.*, **1977**, *16*, 2437.

9 Dewar, M. J. S.; Jie, C.; Yu, J. *Tetrahedron*, **1993**, *49*, 5003.

10 Penner, G. H. *J. Mol. Struct. (THEOCHEM)* **1986**, *137*, 121.

11 Christe, K. O.; Wilson, W.; Wilson, R.; Bau, R.; Feng, J. *J. Am. Chem. Soc.*, **1990**, *112*, 7619.

12 (a) Clark, J. H. *Chem. Rev.*, **1980**, *80*, 429; (b) Yamawaki, J.; Ando, T. *Chem Lett.*, **1979**, 755; (c) Yakobson, G. C.; Akhmetova, N. E. *Synthesis*, **1983**,169; (d) Ando, T.; Brown, S. J.; Clark, J. H.; Cork, D. G.; Hanafusa, T.; Ichihara, J.; Miller, J. M.; Robertson, M. S. *J. Chem. Soc. Perkin Trans. 2*, **1986**, 1133.

13 Moet-Ner (Mautner), M.; Deakyne, C. A. *J. Am. Chem. Soc.*, **1985**, *107*, 469 and 474.

14 Gao, J.; Chou, L. W.; Auerbach, A. *Biophys. J.*, **1993**, *65*, 43.

15 Kim, K. S., Lee, J. Y., Lee, S. J., Ha, T-K. and Kim, D. H. *J. Am. Chem. Soc.*, **1994**, *116*, 7399

16 (a) Sussman, J. L.; Harel, M.; Frolow, F.; Oefner, C.; Goldman, A.; Toker, L.; Silman, I. *Science*, **1991**, *253*, 872; (b) Satow, Y.; Cohen, G. H.; Padlan, E. A.; Davies, D. R. *J. Mol. Biol.*, **1986**, *190*, 593; (c) Pearce, S.; Preston-Hurlburt, P.; Harwot, M. E. *Proc. R. Soc. Lond. (Biol).* **1990**, *241*, 207; (d) Tomaselli, G. F.; Loughlin, J. T.; Harwot, M. E.; Yellen, G. *Biophys. J.*, **1991**, *60*, 721.

17 (a) Petti, M. A.; Shepodd, T. J.; Barrans Jr., R. E.; Dougherty, D. A. *J. Am. Chem. Soc.*, **1988**, *110*, 6825; (b) Stauffer, D. A.; Dougherty, D. A. *Tetrahedron Lett.*, **1988**, *29*, 6039; (c) Dougherty, D. A.; Stauffer, D. A. *Science*, **1990**, *250*, 1558; (d) Stauffer, D. A.; Barrans Jr., R. E.; Dougherty, D. A. *Angew. Chem. Int. Ed. Engl.*, **1990**, *29*, 915.

18 (a) Seppelt, K. *Angew. Chem. Int. Ed. Engl.*, **1992**, *31*, 292; (b) Rieux, C.; Langlois, B.; Gallonew, R. *C. R. Acad. Sci. Paris, t.310, Serie II*, **1990**, 25.

(*Received in UK* 10 *April* 1995; *revised* 19 *June* 1995; *accepted* 23 *June* 1995)